Clinical Biomechanics 33 (2016) 49–54

Contents lists available at ScienceDirect

Clinical Biomechanics

journal homepage: www.elsevier.com/locate/clinbiomech

Immediate effects of modified landing pattern on a probabilistic tibial stress fracture model in runners

T.L. Chen, W.W. An, Z.Y.S. Chan, I.P.H. Au, Z.H. Zhang, R.T.H. Cheung *

Gait & Motion Analysis Laboratory, Department of Rehabilitation Sciences, The Hong Kong Polytechnic University, Hong Kong

ARTICLE INFO

Article history:
Received 20 October 2015
Accepted 17 February 2016

Keywords:
Footstrike
Kinetics
Risk
Modeling

ABSTRACT

Background: Tibial stress fracture is a common injury in runners. This condition has been associated with increased impact loading. Since vertical loading rates are related to the landing pattern, many heelstrike runners attempt to modify their footfalls for a lower risk of tibial stress fracture. Such effect of modified landing pattern remains unknown. This study examined the immediate effects of landing pattern modification on the probability of tibial stress fracture.

Methods: Fourteen experienced heelstrike runners ran on an instrumented treadmill and they were given augmented feedback for landing pattern switch. We measured their running kinematics and kinetics during different landing patterns. Ankle joint contact force and peak tibial strains were estimated using computational models. We used an established mathematical model to determine the effect of landing pattern on stress fracture probability.

Findings: Heelstrike runners experienced greater impact loading immediately after landing pattern switch ($P < 0.004$). There was an increase in the longitudinal ankle joint contact force when they landed with forefoot ($P = 0.003$). However, there was no significant difference in both peak tibial strains and the risk of tibial stress fracture in runners with different landing patterns ($P > 0.986$).

Interpretation: Immediate transitioning of the landing pattern in heelstrike runners may not offer timely protection against tibial stress fracture, despite a reduction of impact loading. Long-term effects of landing pattern switch remains unknown.

1. Introduction

Stress fracture is one of the most common overuse injuries in runners, as it accounts for 6–14% of all running-related musculoskeletal injuries (Bennell et al., 1996; Fredericson et al., 2006; Rauh et al., 2006). The tibia is the most vulnerable site of stress fracture (Milner et al., 2006; Taunton et al., 2002), as 33–55% of the stress fracture incidence rates were related to tibial stress fracture (TSF) (Brukner et al., 1996; Milner et al., 2006). However, the etiology of TSF in runners has yet to be determined Milgrom et al., 2015). Some previous studies suggested that TSF might relate to high vertical loading rates (Crowell et al., 2010; Milner et al., 2006). Some strategies have been shown to effectively reduce impact loading during running and landing pattern modification is one of the most common methods adopted (Cheung and Davis, 2011; Cheung and Rainbow, 2014). Although 75–98% of distance runners land with rearfoot strike (RFS) (Bertelsen et al., 2013; Kasmer et al., 2013; Larson et al., 2011), there is a growing trend to convert landing patterns from RFS to midfoot (MFS) or forefoot strike (FFS) in the running population, partially because of the potential health benefit (Rooney and Derrick, 2013).

Recent studies showed that novice FFS runners might not necessarily exhibit similar biomechanics as habitual FFS runners. After the landing pattern change, some runners may still present vertical impact peak during early stance, which results in high vertical loading rates (An et al., 2015; Cheung and Rainbow, 2014; Valenzuela et al., 2015). Therefore, the immediate effects of landing pattern modification on the risk of TSF in habitual RFS runners remain unknown.

Different landing patterns were reported to alter the ankle joint contact force (AJCF) (Rooney and Derrick, 2013; Sasimontonkul et al., 2007) and possibly alter the risk of TSF by lowering the peak tibia strains (Sasimontonkul et al., 2007). Both mathematical and finite element (FE) models have been used to estimate the risk of TSF (Taylor and Kuiper, 2001; Taylor et al., 1999, 2004). In these models, the fatigue life of the tibia could be determined by the rate of bone damage, repair, and adaptation over a certain period of time, and the accumulative probability of TSF could be quantified.

Hence, this study sought to examine the immediate effects of landing pattern modification on the vertical loading rates, AJCF, peak tibial

* Corresponding author at: ST511, Block S, Department of Rehabilitation Sciences, The Hong Kong Polytechnic University, Hong Kong.
E-mail address: Roy.Cheung@polyu.edu.hk (R.T.H. Cheung).

http://dx.doi.org/10.1016/j.clinbiomech.2016.02.013
0268-0033/

strains, and the risk of TSF. We hypothesized that a lower risk of TSF, accompanied with reduced vertical loading rates, AJCF, and peak tibial strains, would result in a landing pattern switch from RFS to MFS or FFS.

2. Methods

2.1. Subjects

Fourteen experienced shod runners (seven females and seven males; age = 35.3 SD 5.9 years; body height = 1.70 SD 0.08 m; body mass = 64.0 SD 11.2 kg; running experience = 8.4 SD 5.1 years; weekly mileage = 19.9 SD 6.5 km) were recruited from local running clubs. All of the subjects were free from any injury for at least six months prior to the experiment. The experiment protocol was reviewed and approved by the institutional review committee and written consents were obtained prior to the experiment.

2.2. Experimental data collection

Prior to the running evaluation, a single researcher took anthropometric measurements using a caliper and reflective markers were firmly affixed onto selected bony landmarks according to a previously described 6-degree-of-freedom kinematic model (OpenSim model Gait-2392, National Center for Simulation in Rehabilitation Research, Stanford, CA, USA) (Delp et al., 2007). After static calibration of the model, subjects were asked to run at 2.5 m/s on an instrumented treadmill (Tandem treadmill, AMTI, Watertown, MA, USA) with standardized running shoes (Adizero, Adidas, Herogenaurach, Germany). After 5 min of adaptation (Rooney and Derrick, 2013), kinematic and kinetic data from 10 footfalls of the left side were collected and we confirmed all the subjects naturally landed with RFS pattern, as their strike index (SI) was 11.4 SD 8.0% (Cavanagh and Lafortune, 1980). The natural running cadence was also measured in each subject. The subjects were then asked to modify their own landing pattern from RFS to MFS and FFS while running at the same speed and cadence for another 10 min. In order to control step frequency, a metronome was used to provide feedback of his/her natural running cadence during running with RFS landing. In addition, in order to facilitate landing pattern switch, real-time visual feedback of the landing pattern was provided by a monitor placed in front of the treadmill. We collected 10 MFS and 10 FFS footfalls on the left side, which first appeared in the 10-minute running bout during offline analysis. SI of the 10 footfalls for the two non-RFS conditions was also calculated for verification.

2.3. Data processing

Marker trajectories were collected using an 8-camera motion capture system (Vicon, Oxford Metrics Group, Oxford, UK) at 160 Hz. Ground reaction force (GRF) and moment data were sampled at 1600 Hz. Kinematic and kinetic data were filtered using a fourth-order zero-lag Butterworth filter with a lowpass frequency of 8 and 50 Hz, respectively (Edwards et al., 2011; Laughton et al., 2003). We measured average (VALR) and instantaneous vertical loading rates (VILR) with the established method (An et al., 2015). In brief, VALR is the slope of the line through the 20% point and the 80% point of the vertical impact peak and VILR is the maximum slope of the vertical ground reaction force curve between successive data points in the same region.

2.4. Musculoskeletal modeling

OpenSim 3.3 (National Center for Simulation in Rehabilitation Research, Stanford, CA, USA) was used to perform biomechanical simulation. Data from the Vicon system were adjusted to OpenSim environment using open-source toolkit (Gait Extract Toolbox for Matlab, Version 1.71). The full-body kinematic model was then scaled to accommodate the individual anthropometry based on marker positions obtained in the static trial (Delp et al., 2007). This model features 23-degree-of-freedom and 92 musculotendon actuators representing 76 muscles in the lower extremities and torso (OpenSim Documentation, 2013). In each subject, the kinematics and kinetics were used in subsequent calculation of individual muscle force (Donnelly et al., 2012; Lewis and Garibay, 2015). Ankle joint reaction force (AJCF) was then calculated as the sum of the muscle forces spanning the ankle joint and the ankle joint reaction force in the three orthogonal directions (Knarr and Higginson, 2015; Rooney and Derrick, 2013). A total of 12 muscles were selected for the force prediction. They were medial and lateral gastrocnemious, soleus, tibialis anterior, tibialis posterior, peroneus longus, peroneus brevis, peroneus tertius, extensor digitorum longus, extensor hallucis longus, flexor hallucis longus, and flexor digitorum longus. In this study, the direction of each selected muscle force in the tibia frame was obtained using an OpenSim plugin (van Arkel et al., 2013).

2.5. Finite element modeling

Abaqus 6.13 (Dassault Systèmes Simulia Corp., Providence, USA) was used to perform the finite element (FE) analysis. Tibia was modeled based on an online available database (VAKHUM dataset, 2003). The material-mapping and hexa-meshed model of a sample left tibia was used in this study. Its material properties were assumed to be linear elastic and isotropic, with cortical bone having an average Young's modulus of 17.19 GPa, and trabecular bone of 10.69 GPa. A Poisson's ratio of 0.3 was consistent throughout the entire model. A sensitivity analysis was performed to determine mesh size for the study. Five different mesh densities (6.4, 5.5, 3.6, 2.7, and 2.0 mm) were investigated and an average change of <5% in the solution output (strain value of each element group) was considered adequate to ensure completed mesh convergence (Anderson et al., 2007; Henninger et al., 2010). The model was further validated by performing linear regression analysis of the principal strains predicted by the FE method and measured strains reported in previous in-vitro studies, one of which used cadaveric tibia and another used composite tibia (Completo et al., 2007; Mir et al., 2013). The regression parameters (slope, intercept, and R^2) were reported and the root mean square error as a percentage of the peak measured principal strain (RMSE %) was also calculated to demonstrate the accuracy of the FE model.

In the simulation, the model was orthogonally oriented which was consistent with the OpenSim environment (OpenSim Documentation, 2013; VAKHUM dataset, 2003). A separated tibia model was created for each subject scaled longitudinally and radially to his/her tibial geometry and body mass (Edwards et al., 2009, 2010). Each model was fully constrained at the tibial plateau and a distributed AJCF was applied to the distal tibia (Edwards et al., 2009). On the basis of a previous study (Sasimontonkul et al., 2007), 10% of the AJCF was borne by the fibula. Therefore, AJCF on the tibia was calculated as follows:

$$F_c^t = 0.9.\left[RF^t + \sum_{i=1}^{12} f_i\right]$$

where F_c^t was the three components of AJCF acting on the tibia, RF^t represented the three components of ankle joint reaction force, and f_i represented the three components of the ith predicted muscle force crossing the ankle joint (selected muscle number = 12).

We assumed that the tibia was operating within its elastic range during the impact, and the maximal principle strain and volume for each element was exported after loading completed. We divided elements experiencing similar strains and found that eight groups were sufficient to identify inter-group differences without significant error (Taylor and Kuiper, 2001). The corresponding element volumes for each group were calculated by summing individual element volume constituting the group. Strain values from the mid-point were used to represent the

Table 1
Sensitivity analysis of FE model mesh size.

Average mesh size (mm)	Mid-point strain value in each element group (με)								Average solution change (%)
	1	2	3	4	5	6	7	8	
6.5 × 6.5	2497.50	1250.64	850.99	614.98	484.92	361.65	272.61	158.72	
5.5 × 5.5	2459.82	1281.64	902.77	642.54	499.09	378.96	253.58	138.87	5.22
3.6 × 3.6	2315.99	1209.07	831.50	581.97	455.14	345.17	235.90	132.87	7.23
2.7 × 2.7	2505.91	1237.93	851.73	606.78	468.04	354.70	243.06	137.29	3.66
2.0 × 2.0	2475.24	1284.71	892.89	632.70	492.48	373.63	255.70	135.29	3.92

strain level of each group for subsequent calculation (Edwards et al., 2009, 2010).

2.6. Mathematical probabilistic model of stress fracture

The probability of TSF was determined using a mathematical model developed in the previous studies (Taylor and Kuiper, 2001; Taylor et al., 1999, 2004). In brief, the model introduced an algorithm to predict accumulative probability of TSF over a fixed time period involving bone adaptation, fatigue, and repair. According to an in-vitro study (Turner et al., 1994), bone adaption was taken into account by assuming a maximal rate of lamellar bone deposition of 4 μm/day on the periosteal surface. Therefore, the time-dependent strain value was calculated using equation of beam theory. An equivalent strain value for each element group was computed representing the strain level over a fixed period of time by (Carter and Caler, 1983; Carter et al., 1981; Taylor et al., 2004):

$$\Delta\varepsilon_{eq} = \left(\frac{1}{t_T}\int_0^{t_T}\Delta\varepsilon^{6.6}dt\right)^{1/6.6}$$

where t_T represented the total time over which adaptation took place (Taylor et al., 2004). In this study, we simulated a period of 100 days. This duration was able to cover the period of TSF incidence reported in the previous studies (Edwards et al., 2009, 2010).

The fatigue life of the tibia (N_f) was determined using the standard fatigue equation (Carter et al., 1981):

$$N_f = 2.94\Delta\varepsilon_{eq}^{-6.6}\times 10^{-9}$$

For *in-vivo* application, $\Delta\varepsilon$ represented the maximal strain range that the tibia withstood. We used the modified Weibull equation to measure the fatigue life of the tibia (Taylor and Kuiper, 2001; Weibull, 1951) as follows:

$$P_{fs} = 1 - exp\left[-\left(\frac{V_s}{V_{so}}\right)\left(\frac{t}{t_f}\right)^{1.2}\right]$$

where t_f and V_{so} were reference time and volume derived from a previous study (Taylor et al., 2004). t represented the computed time to fatigue for a fixed strain range, which was equal to the fatigue life divided by subject-specific cycles per day (Taylor et al., 2004). Subject-specific cycle was determined by the natural cadence measured and the reported weekly running mileage of individual subject. V_s and P_{fs} represented the volume of each element group and their respective cumulative probability of bone failure. Since P_{fs} of individual element groups were not constant throughout the entire bone, the cumulative probability of bone failure P_f for the whole tibia was calculated as:

$$P_f = 1-(1-P_1)(1-P_2)(1-P_3)\ldots(1-P_k)$$

In order to estimate the probability of failure with the consideration of bone repair, the probability density function of failure (Q_f) was determined. (Q_f)represented the instantaneous fatigue probability occurring in a particular time period (such as a given day) and it was expressed as

$$Q_f = \frac{dP_f}{dt}.$$

Bone repair was incorporated into the model with the use of a second Weibull equation (Taylor et al., 2004):

$$P_r = 1 - exp\left[-\left(\frac{t}{26}\right)^2\right]$$

where P_r represented the cumulative probability of bone repair over a certain period of time. Stress fracture is a time-dependent procedure involving both fatigue and repair. The bone would not fail if sufficient time was allowed for repair. Therefore, the instantaneous probability of stress fracture within a unit period was calculated as

$$Q_{fr} = Q_f(1-P_r).$$

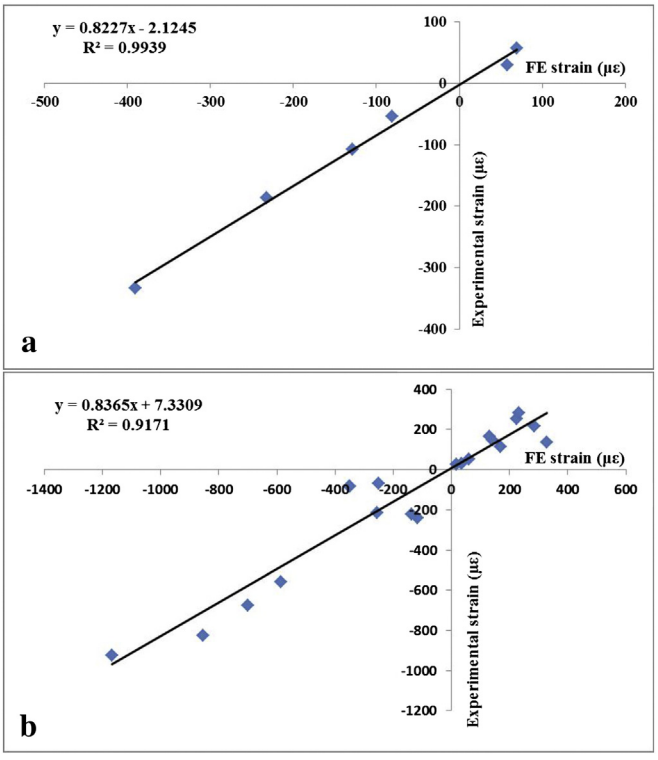

Fig. 1. Linear regression between experimental and FE principal strains in (a) comparison with Mir et al., 2013; and (b) comparison with Completo et al., 2007.

Table 2
Strike indices of the participants during running trials with different landing patterns.

Characteristics	Mean (SD)
Strike index during RFS (%)	11.42 (7.98)
Strike index during MFS (%)	57.06 (6.02)
Strike index during FFS (%)	73.89 (4.85)

Hence, the cumulative probability of TSF (P_{fr}) with repair was calculated as

$$P_{fr} = \int_0^t Q_{fr} dt.$$

2.7. Statistical analysis

VALR, VILR, peak AJCF, peak tibial strains, and accumulative probability of TSF over 100 days were compared between different landing patterns using one-way ANOVA. Post-hoc comparison was conducted using LSD analyses, if necessary. Statistical analysis was performed in SPSS (SPSS, Inc., Chicago, IL, USA) with the global alpha set at 0.05.

3. Results

The sensitivity analysis of mesh size is displayed in Table 1. It was shown that a 2.7 mm mesh provided sufficient resolution for completed mesh convergence (Akbarshahi et al., 2014). In this study, the FE model of tibia contained 26,508 elements (type C3D8I) and 30,002 nodes. Very congruent results were obtained by simulating the tibia loading using our FE model (Fig. 1). The regression line of principal strain values predicted by our FE model versus experimental principal strain values had a slope of 0.82 (Mir et al., 2013) and 0.84 (Completo et al., 2007). The R^2 and RMSE were 0.92–0.99 and 2.7–8.6%, respectively, and overall all the values predicted by our FE model were in good agreement with the experimentally measured strain values (Akbarshahi et al., 2014; Completo et al., 2013; Gray et al., 2008).

As indicated by the corresponding SI (Table 2), all the subjects were able to adjust their landing patterns with augmented biofeedback. We found significant differences in both VALR and VILR between different landing patterns ($P < 0.001$) (Table 3). Post-hoc analysis indicated that VALR and VILR were significantly higher during RFS than MFS or FFS ($P < 0.004$). Three orthogonal directions of AJCF are shown in Table 3. We found significant differences in the longitudinal AJCF between different landing patterns ($P = 0.011$) and in the post-hoc analyses, longitudinal AJCF during FFS was significantly greater than RFS ($P = 0.003$). However, there was no significant difference in both anteroposterior ($P = 0.966$) and mediolateral AJCF ($P = 0.219$) across landing patterns.

The FE analysis is graphically presented in Fig. 2. There were no significant differences in the peak tibial strains between different landing conditions ($P = 0.864$) (Table 3). Accumulative probability of TSF in runners with different landing patterns are plotted in the function of time over 100 days (Fig. 3). Regardless of landing patterns, the probability of TSF increased with the number of running days and it leveled off at around 40 days after commencement. Statistically, the risk of TSF was similar in runners with RFS, MFS, or FFS at the 100th day of running ($P = 0.956$).

4. Discussion

This study sought to compare the accumulative probability of TSF in runners with RFS, MFS, and FFS. When compared with RFS, the vertical loading rates were reduced when the runners landed with MFS or FFS. Although there were some noticeable changes in the AJCF after landing pattern modification, such differences did not lower peak tibial strains and the risks of TSF.

In this study, we recruited a group of experienced runners who habitually landed with RFS for two reasons. First, they are the majority of the running population (Bertelsen et al., 2013; Kasmer et al., 2013; Larson et al., 2011) and the findings could be better generalized. Second, with the recent better awareness of the potential health benefits by landing pattern modification, habitual RFS runners are more likely than those MFS or FFS runners to consider a landing pattern switch.

In accord with previous gait retraining studies (Cheung and Davis, 2011; Crowell and Davis, 2011; Crowell et al., 2010), the subjects were able to alter their running mechanics with the biofeedback provided. Following the landing pattern transition from RFS to MFS or FFS, the VALR and VILR were reduced by 17–68% and 13–62% respectively, which was comparable to previous findings (15–39% in VALR and 16–39% in VILR) (Crowell and Davis, 2011).

Originally, we expected that lower vertical loading rates during non-RFS landing would reduce the risk of TSF by lowering the AJCF and peak tibial strains. AJCF is the internal loads that may create damage (Winter, 2009). In our study, the longitudinal AJCF during running was relatively smaller than previous studies, which could be explained by the slower testing speeds in the present study. For instance, Giltsch and Bauman reported up to 12 body weights of longitudinal AJCF when the subjects were running at 5.0 m/s (Glitsch and Baumann, 1997). Similarly, a longitudinal AJCF of 9.0 body weights was reported in another running experiment at 3.84 m/s (Sasimontonkul et al., 2007). We selected the current testing speed because it was found as the average usual speed in our sample during a pilot study. Lower vertical loading rates did not lead to a smaller longitudinal AJCF when the subjects altered their landing pattern from RFS to FFS. Instead, we found a reversed pattern and the reasons could be two-fold. First, the vertical loading rates occur in the early stance but the peak AJCF occurs during mid stance (Sasimontonkul et al., 2007). Second, it has been reported that during non-RFS running, the muscle force required by the ankle plantarflexors would be increased (Rooney and Derrick, 2013; Yong et al., 2014). Extra internal muscle force may lead to an increase of tibial compression (Sasimontonkul et al., 2007). Conversely, we failed to find any difference in the shear force at the ankle joint across landing patterns. Shear loading of the distal tibia and internal muscle forces were in opposite directions during stance phase of running (Sasimontonkul et al., 2007) and net shear force may be counterbalanced by the increased muscle force during non-RFS landing.

Table 3
Mean (SD) vertical loading rates, ankle joint contact forces, peak tibial strain, and probability of tibial stress fracture across landing patterns.

	RFS Mean (SD)	MFS Mean (SD)	FFS Mean (SD)	*P*
VALR (BW/s)	65.65 (7.94)	40.06 (9.10)	35.00 (6.84)	<0.001
VILR (BW/s)	91.16 (10.21)	60.75 (12.08)	51.07 (8.60)	<0.001
Anteroposterior AJCF (BW)	0.78 (0.14)	0.79 (0.12)	0.78 (0.14)	0.966
Longitudinal AJCF (BW)	5.45 (0.82)	5.96 (0.78)	6.52 (1.03)	0.011
Mediolateral AJCF (BW)	0.17 (0.06)	0.14 (0.07)	0.12 (0.09)	0.219
Peak tibial strain (με)	7939.79 (1588.74)	7932.07 (1389.12)	7840.40 (1583.39)	0.864
Probability of TSF (%)	14.15 (19.54)	12.23 (15.73)	13.89 (19.50)	0.956

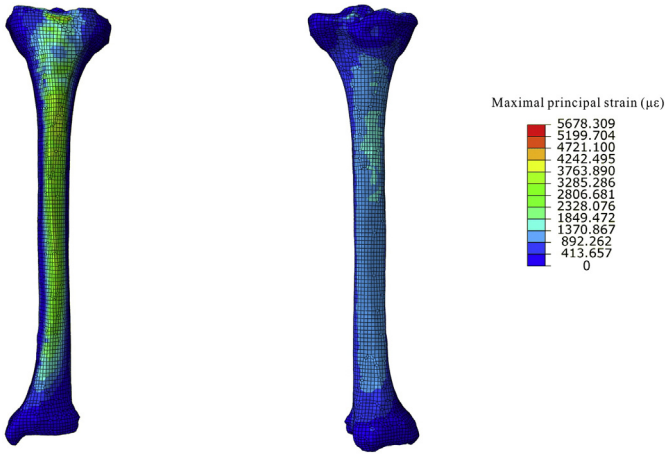

Fig. 2. Sagittal views of a representative finite element model of the tibia displaying maximal principal strain (με) during running. The models were loaded in bending and axial compression with tension on the anterior surface (left) and compression on the posterior surface (right).

Under compression and posterior bending during most of the stance, our tibia model exhibited a greater tensile strain on the anterior than posterior surface. This finding was in accord with previous clinical trials (Boyer et al., 2014; Williams et al., 2010) but different from some simulation studies (Edwards et al., 2009, 2010). Such difference may be caused by the material properties that we used in the FE analysis. Our tibia model contained more trabecular bone in the shaft than the models used in those previous studies and it was thus more resistant to bending. Besides, tibia is characterized by triangular cross-section area in the shaft which features sharp border along the anterior crest (Gray, 2011). Therefore, our findings were in accord with previous clinical reports that anterior crest is a common site for TSF (Blackman, 2010; Brukner and Bennell, 1997; Rettig et al., 1988). Since the AJCF only subtly responded to the changed landing pattern, we did not find significant immediate effects of landing pattern modification on the peak tibial strains.

The accumulative probability of TSF across RFS, MFS, and FFS was 12–14% on approximately 40 days, which found similarity to previous clinical trials (Changstrom et al., 2015; Sharma et al., 2015) and computational predictions (Edwards et al., 2009, 2010). However, there was no significant difference in the TSF risk between RFS, MFS, and FFS. This observation could be explained by the biomechanical difference across landing patterns. One of the most distinctive features between RFS and non-RFS was the presence/absence of the vertical impact peak during early stance (Lieberman et al., 2010). However, the algorithm we used to estimate the tibial loading was more related to active peak, i.e. the maximum loading during stance, than the vertical impact peak (Rooney and Derrick, 2013), landing pattern modification may not provide protection against TSF, at least in the perspective of computation estimation. The clinical evidence of the purported health benefits of non-RFS landing (Davis et al., 2004; Milner et al., 2006) could be related to some other factors that associated with the altered landing patterns. In this study, running speed and cadence remained constant during the evaluation. It indicated that runners were running with different landing patterns at the same speed and with unchanged stride length. It has been well noted that FFS runners tended to exhibit increased cadence and reduced stride length (Bertelsen et al., 2013; Kulmala et al., 2013; Willson et al., 2015). While the effects of running speed was shown to be more significant, reducing stride length could lower the TSF risk by 3–6% (Edwards et al., 2009, 2010)

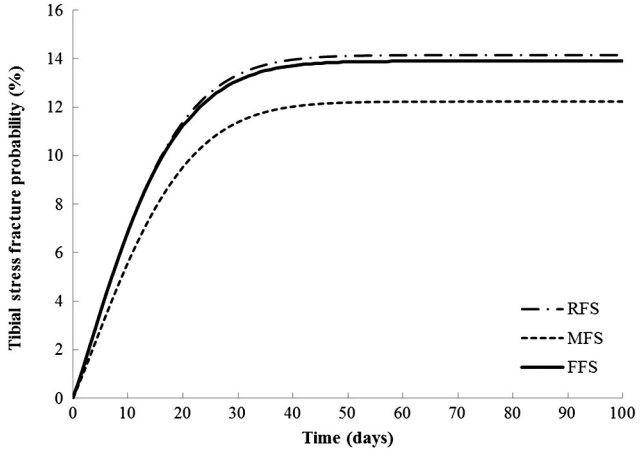

Fig. 3. Accumulative probability of tibial stress fracture.

Several limitations should be addressed in light of the findings presented. First, the running speed in the evaluation was slow. Therefore, our findings may not be able to generalize to runners with faster pacing. Second, although our FE model was scaled to subjects' individual segment size, subject-specific bone morphologies and material properties were not considered. Since bone quality is a contributing factor of TSF, a generic FE model used in this study may not predict individualized risk. Third, the long-term effect of landing pattern modification was not examined in this study. In contrast to previous gait retraining studies, our subjects did not receive a systematic training and the reduction in the vertical loading rates could be temporary. Finally, we assumed that the running mechanics would remain unchanged during the 100-day exposure period. Therefore, the long-term effects of the landing pattern switch in runners who undergo a systemic gait retraining may be different from our findings.

5. Conclusions

Our findings suggested that habitual RFS runners should not expect a reduction of TSF risk immediately after a landing pattern transition, although we observed a lower impact loading when RFS runners landed with non-RFS. Long term effects of landing pattern switch remains unknown.

References

Akbarshahi, M., Fernandez, J.W., Schache, A.G., Pandy, M.G., 2014. Subject-specific evaluation of patellofemoral joint biomechanics during functional activity. Med. Eng. Phys. 36, 1122–1133. http://dx.doi.org/10.1016/j.medengphy.2014.06.009.

An, W., Rainbow, M.J., Cheung, R.T.H., 2015. Effects of surface inclination on the vertical loading rates and landing pattern during the first attempt of barefoot running in habitual shod runners. Bio. Med. Res. Int. 2015, 240153. http://dx.doi.org/10.1155/2015/240153.

Anderson, A.E., Ellis, B.J., Weiss, J.A., 2007. Verification, validation and sensitivity studies in computational biomechanics. Comput. Methods Biomech. Biomed. Engin. 10, 171–184. http://dx.doi.org/10.1080/10255840601160484.

Bennell, K.L., Malcolm, S.A., Thomas, S.A., Wark, J.D., Brukner, P.D., 1996. The incidence and distribution of stress fractures in competitive track and field athletes. A twelve-month prospective study. Am. J. Sports Med. 24, 211–217.

Bertelsen, M.L., Jensen, J.F., Nielsen, M.H., Nielsen, R.O., Rasmussen, S., 2013. Footstrike patterns among novice runners wearing a conventional, neutral running shoe. Gait Posture 38, 354–356. http://dx.doi.org/10.1016/j.gaitpost.2012.11.022.

Blackman, P., 2010. Shin pain in athletes: assessment and management. Aust. Fam. Physician 39, 24.

Boyer, E.R., Rooney, B.D., Derrick, T.R., 2014. Rearfoot and midfoot or forefoot impacts in habitually shod runners. Med. Sci. Sports Exerc. 46, 1384–1391. http://dx.doi.org/10.1249/MSS.0000000000000234.

Brukner, P., Bennell, K., 1997. Stress fractures in female athletes. Diagnosis, management and rehabilitation. Sports Med. Auckl. NZ 24, 419–429.

Brukner, P., Bradshaw, C., Khan, K.M., White, S., Crossley, K., 1996. Stress fractures: a review of 180 cases. Clin. J. Sport Med. Off. J. Can. Acad. Sport Med. 6, 85–89.

Carter, D.R., Caler, W.E., 1983. Cycle-dependent and time-dependent bone fracture with repeated loading. J. Biomech. Eng. 105, 166–170.

Carter, D.R., Caler, W.E., Spengler, D.M., Frankel, V.H., 1981. Fatigue behavior of adult cortical bone: the influence of mean strain and strain range. Acta Orthop. 52, 481–490.

Cavanagh, P.R., Lafortune, M.A., 1980. Ground reaction forces in distance running. J. Biomech. 13, 397–406.

Changstrom, B.G., Brou, L., Khodaee, M., Braund, C., Comstock, R.D., 2015. Epidemiology of stress fracture injuries among US high school athletes, 2005-2006 through 2012–2013. Am. J. Sports Med. 43, 26–33. http://dx.doi.org/10.1177/0363546514562739.
Cheung, R.T.H., Davis, I.S., 2011. Landing pattern modification to improve patellofemoral pain in runners: a case series. J. Orthop. Sports Phys. Ther. 41, 914–919. http://dx.doi.org/10.2519/jospt.2011.3771.
Cheung, R.T.H., Rainbow, M.J., 2014. Landing pattern and vertical loading rates during first attempt of barefoot running in habitual shod runners. Hum. Mov. Sci. 34, 120–127. http://dx.doi.org/10.1016/j.humov.2014.01.006.
Completo, A., Fonseca, F., Simões, J.A., 2007. Finite element and experimental cortex strains of the intact and implanted tibia. J. Biomech. Eng. 129, 791. http://dx.doi.org/10.1115/1.2768382.
Completo, A., Duarte, R., Fonseca, F., Simões, J.A., Ramos, A., Relvas, C., 2013. Biomechanical evaluation of different reconstructive techniques of proximal tibia in revision total knee arthroplasty: an in-vitro and finite element analysis. Clin. Biomech. 28, 291–298. http://dx.doi.org/10.1016/j.clinbiomech.2012.12.009.
Crowell, H.P., Davis, I.S., 2011. Gait retraining to reduce lower extremity loading in runners. Clin. Biomech. 26, 78–83. http://dx.doi.org/10.1016/j.clinbiomech.2010.09.003.
Crowell, H.P., Milner, C.E., Hamill, J., Davis, I.S., 2010. Reducing impact loading during running with the use of real-time visual feedback. J. Orthop. Sports Phys. Ther. 40, 206–213. http://dx.doi.org/10.2519/jospt.2010.3166.
Davis, I., Milner, C.E., Hamill, J., 2004. Does increased loading during running lead to tibial stress fractures? A prospective study. Med. Sci. Sports Exerc. 35, 58.
Delp, S.L., Anderson, F.C., Arnold, A.S., Loan, P., Habib, A., John, C.T., Guendelman, E., Thelen, D.G., 2007. OpenSim: Open-source software to create and analyze dynamic simulations of movement. IEEE Trans. Biomed. Eng. 54, 1940–1950. http://dx.doi.org/10.1109/TBME.2007.901024.
Donnelly, C.J., Lloyd, D.G., Elliott, B.C., Reinbolt, J.A., 2012. Optimizing whole-body kinematics to minimize valgus knee loading during sidestepping: implications for ACL injury risk. J. Biomech. 45, 1491–1497. http://dx.doi.org/10.1016/j.jbiomech.2012.02.010.
Edwards, W.B., Taylor, D., Rudolphi, T.J., Gillette, J.C., Derrick, T.R., 2009. Effects of stride length and running mileage on a probabilistic stress fracture model. Med. Sci. Sports Exerc. 41, 2177–2184. http://dx.doi.org/10.1249/MSS.0b013e3181a984c4.
Edwards, W.B., Taylor, D., Rudolphi, T.J., Gillette, J.C., Derrick, T.R., 2010. Effects of running speed on a probabilistic stress fracture model. Clin. Biomech. 25, 372–377. http://dx.doi.org/10.1016/j.clinbiomech.2010.01.001.
Edwards, W.B., Troy, K.L., Derrick, T.R., 2011. On the filtering of intersegmental loads during running. Gait Posture 34, 435–438. http://dx.doi.org/10.1016/j.gaitpost.2011.06.006.
Fredericson, M., Jennings, F., Beaulieu, C., Matheson, G.O., 2006. Stress fractures in athletes. Top. Magn. Reson. Imaging TMRI 17, 309–325. http://dx.doi.org/10.1097/RMR.0b013e3180421c8c.
Glitsch, U., Baumann, W., 1997. The three-dimensional determination of internal loads in the lower extremity. J. Biomech. 30, 1123–1131.
Gray, S., 2011. Gray's Anatomy. Knopf Doubleday Publishing Group.
Gray, H.A., Taddei, F., Zavatsky, A.B., Cristofolini, L., Gill, H.S., 2008. Experimental validation of a finite element model of a human cadaveric tibia. J. Biomech. Eng. 130, 031016. http://dx.doi.org/10.1115/1.2913335.
Henninger, H.B., Reese, S.P., Anderson, A.E., Weiss, J.A., 2010. Validation of computational models in biomechanics. Proc. Inst. Mech. Eng. [H] 224, 801–812.
Kasmer, M.E., Liu, X.-C., Roberts, K.G., Valadao, J.M., 2013. Foot-strike pattern and performance in a marathon. Int. J. Sports Physiol. Perform. 8, 286–292.
Knarr, B.A., Higginson, J.S., 2015. Practical approach to subject-specific estimation of knee joint contact force. J. Biomech. 48, 2897–2902. http://dx.doi.org/10.1016/j.jbiomech.2015.04.020.
Kulmala, J.-P., Avela, J., Pasanen, K., Parkkari, J., 2013. Forefoot strikers exhibit lower running-induced knee loading than rearfoot strikers: med. Sci. Sports Exerc. 45, 2306–2313. http://dx.doi.org/10.1249/MSS.0b013e31829efcf7.
Larson, P., Higgins, E., Kaminski, J., Decker, T., Preble, J., Lyons, D., McIntyre, K., Normile, A., 2011. Foot strike patterns of recreational and sub-elite runners in a long-distance road race. J. Sports Sci. 29, 1665–1673. http://dx.doi.org/10.1080/02640414.2011.610347.
Laughton, C.A., Davis, I.M., Hamill, J., 2003. Effect of strike pattern and orthotic intervention on tibial shock during running. J. Appl. Biomech. 19, 153–168.
Lewis, C.L., Garibay, E.J., 2015. Effect of increased pushoff during gait on hip joint forces. J. Biomech. 48, 181–185. http://dx.doi.org/10.1016/j.jbiomech.2014.10.033.
Lieberman, D.E., Venkadesan, M., Werbel, W.A., Daoud, A.I., D'Andrea, S., Davis, I.S., Mang'eni, R.O., Pitsiladis, Y., 2010. Foot strike patterns and collision forces in habitually barefoot versus shod runners. Nature 463, 531–535. http://dx.doi.org/10.1038/nature08723.
Milgrom, C., Burr, D.B., Finestone, A.S., Voloshin, A., 2015. Understanding the etiology of the posteromedial tibial stress fracture. Bone 78, 11–14. http://dx.doi.org/10.1016/j.bone.2015.04.033.
Milner, C.E., Ferber, R., Pollard, C.D., Hamill, J., Davis, I.S., 2006. Biomechanical factors associated with tibial stress fracture in female runners: med. Sci. Sports Exerc. 38, 323–328. http://dx.doi.org/10.1249/01.mss.0000183477.75808.92.
Mir, H.R., Marinescu, R.C., Janda, H., Russell, T.A., 2013. Biomechanical effects of the nail entry zone and anterior cortical bone loss on the proximal tibia. J. Orthop. Trauma 27, 34–41.
Rauh, M.J., Macera, C.A., Trone, D.W., Shaffer, R.A., Brodine, S.K., 2006. Epidemiology of stress fracture and lower-extremity overuse injury in female recruits. Med. Sci. Sports Exerc. 38, 1571–1577. http://dx.doi.org/10.1249/01.mss.0000227543.51293.9d.
Rettig, A.C., Shelbourne, K.D., McCarroll, J.R., Bisesi, M., Watts, J., 1988. The natural history and treatment of delayed union stress fractures of the anterior cortex of the tibia. Am. J. Sports Med. 16, 250–255.
Rooney, B.D., Derrick, T.R., 2013. Joint contact loading in forefoot and rearfoot strike patterns during running. J. Biomech. 46, 2201–2206. http://dx.doi.org/10.1016/j.jbiomech.2013.06.022.
Sasimontonkul, S., Bay, B.K., Pavol, M.J., 2007. Bone contact forces on the distal tibia during the stance phase of running. J. Biomech. 40, 3503–3509. http://dx.doi.org/10.1016/j.jbiomech.2007.05.024.
Sharma, J., Greeves, J.P., Byers, M., Bennett, A.N., Spears, I.R., 2015. Musculoskeletal injuries in British Army recruits: a prospective study of diagnosis-specific incidence and rehabilitation times. BMC Musculoskelet. Disord. 16, 106. http://dx.doi.org/10.1186/s12891-015-0558-6.
Taunton, J.E., Ryan, M.B., Clement, D.B., McKenzie, D.C., Lloyd-Smith, D.R., Zumbo, B.D., 2002. A retrospective case–control analysis of 2002 running injuries. Br. J. Sports Med. 36, 95–101.
Taylor, D., Kuiper, J.H., 2001. The prediction of stress fractures using a “stressed volume” concept. J. Orthop. Res. Off. Publ. Orthop. Res. Soc. 19, 919–926. http://dx.doi.org/10.1016/S0736-0266(01)00009-2.
Taylor, D., O'Brien, F., Prina-Mello, A., Ryan, C., O'Reilly, P., Lee, T.C., 1999. Compression data on bovine bone con" rms that astressed volumea principle explains the variability of fatigue strength results. J. Biomech. 32, 1203.
Taylor, D., Casolari, E., Bignardi, C., 2004. Predicting stress fractures using a probabilistic model of damage, repair and adaptation. J. Orthop. Res. 22, 487–494. http://dx.doi.org/10.1016/j.orthres.2003.08.022.
Turner, C.H., Forwood, M.R., Rho, J.Y., Yoshikawa, T., 1994. Mechanical loading thresholds for lamellar and woven bone formation. J. Bone Miner. Res. Off. J. Am. Soc. Bone Miner. Res. 9, 87–97. http://dx.doi.org/10.1002/jbmr.5650090113.
Valenzuela, K.A., Lynn, S.K., Mikelson, L.R., Noffal, G.J., Judelson, D.A., 2015. Effect of acute alterations in foot strike patterns during running on sagittal plane lower limb kinematics and kinetics. J. Sports Sci. Med. 14, 225.
van Arkel, R.J., Modenese, L., Phillips, A.T.M., Jeffers, J.R.T., 2013. Hip abduction can prevent posterior edge loading of hip replacements: HIP ABDUCTION PREVENTS EDGE LOADING. J. Orthop. Res. 31, 1172–1179. http://dx.doi.org/10.1002/jor.22364.
Weibull, W., 1951. A Statistical Distribution Function of Wide Applicability. pp. 293–297.
Williams, D.S., McClay, I.S., Manal, K.T., 2010. Lower extremity mechanics in runners with a converted forefoot strike pattern [WWW Document]. Hum. Kinet. J. (URL http://journals.humankinetics.com/jab-back-issues/jabvolume16issue2may/lower-extremity-mechanics-in-runners-with-a-converted-forefoot-strike-pattern accessed 9.9.15).
Willson, J.D., Ratcliff, O.M., Meardon, S.A., Willy, R.W., 2015. Influence of step length and landing pattern on patellofemoral joint kinetics during running. Scand. J. Med. Sci. Sports http://dx.doi.org/10.1111/sms.12383.
Winter, D.A., 2009. Biomechanics and Motor Control of Human Movement. John Wiley & Sons.
Yong, J.R., Silder, A., Delp, S.L., 2014. Differences in muscle activity between natural forefoot and rearfoot strikers during running. J. Biomech. 47, 3593–3597. http://dx.doi.org/10.1016/j.jbiomech.2014.10.015.

Web references

OpenSim Documentation, 2013. Available: http://simtk-confluence.stanford.edu:8080/display/OpenSim/OpenSim+Support (Last accessed 25 March 2015).
VAKHUM dataset, 2003. Available http://www.ulb.ac.be/project/vakhum/ (Last accessed 25 March 2015).